

Symmetry of Turbulent Characteristics Inside Urban Intersection

Radka Kellnerová^{1,2}

Zbyněk Jaňour¹

¹ Institute of Thermomechanics, Academy of Science of the Czech Republic, Prague, Czech Republic *

² Department of Meteorology and Environment Protection, Charles University, Prague, Czech Republic

Introduction

Physical modeling is one of the appropriate methods for investigation of dispersion and flow processes inside the built-up area. This method is based on wind-tunnel simulation. The flow conditions created in the tunnel are geometrically and dynamically similar to the ones we can observe in the atmosphere.

The construction of wind-tunnel determines the range of cases we are able to simulate. The vertical extension of model have to respect vertical depth of artificial boundary layer. The maximal horizontal extent of researched area depends on the horizontal dimension of tunnel working section. With regard to the characteristics of inlet boundary layer, especially the roughness length z_0 (Jensen, 1958), the scale of model have to be chosen properly.

In wind-tunnel modeling a lot of embarrassments are related to the central symmetry. Even a small asymmetry in flow field leads to a significant change in pollutant dispersion, therefore the concentration field is very sensitive to the symmetry of set-up. The asymmetry of flow field inside the symmetrical model is often caused by one of two reasons: inappropriate inlet conditions or non-symmetric set-up of model.

The aim of this research was to estimate flow processes inside the wind-tunnel, mainly to investigate the symmetry over all working space and the influence of dimension of model relative to the dimension of working section.

Experimental Set-up

The experiment have been conducted in open-circuit low-speed aerodynamic tunnel belonging in to Institute of Thermomechanics in Nový Knín, Czech Republic (see scheme in Figure 1). The tunnel has a 20,5 m long developing section opening with spires and roughness elements installed on the whole floor. The elements have staggered set-up with 5 and 10 cm high sheets. At the beginning of working section the character of boundary layer is analogous to the real downtown boundary layer according to Snyder's classification (1981). The available reducing for scaling factor of models lies between 1:100 and 1:400. The thickness of turbulent layer attains 75 cm.

The tunnel construction is three times bent along its length. The first two bends are central symmetrical with respect to the developing section. The first one changes the vertical flow into the horizontal flow in the mouth of tube. Second one is located behind the working section and it re-changes the horizontal direction back to the vertical. The third bend veers the wind by 90° to the left and brings the air out of the tunnel.

The dimension of testing cross-section is 1,5 m x 1,5 m. The sector available for measurement is 2 m long and it is covered with 3-D traverse system with resolution of 1 mm. The coordinates origin lies in the middle of working section.

The flow measurements were carried out using two-dimensional fibre-optic laser Doppler anemometry (LDA). The glycerine droplets - for potency of tracing by laser - were added to the main flow. Droplets with mean radius 1 μm passively flow in the air with sufficiently low sedimentation velocity (approximately 0.02 $\text{m}\cdot\text{s}^{-1}$).

LDA data rate above the obstacle level reaches approximately 200 Hz with averaging time 100 s. Inside the urban canopy data rate decreases to 70-100 Hz, due to poor availability of glycerine fog behind the obstacles. The acquisition time was hence extended to 120 s. The reference velocity was obtained from hot-wire anemometer mounted in the tunnel axis.

*radka.kellnerova@email.cz, Dolejšková 1402/5, Praha 8, 182 00

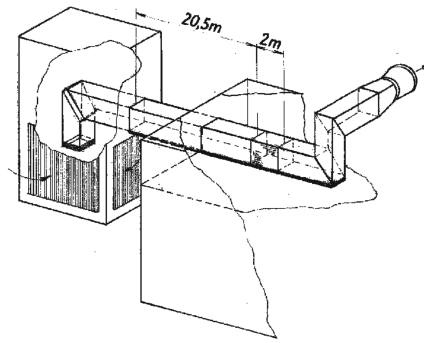


Figure 1: Scheme of tunnel.

For "empty tunnel" arrangement, only roughness elements were put on the testing floor with the same sequencing as the one we used in the developing zone (Figure 2 - left).

The model setting was designed after the typical inner-city area with 20 m high apartment houses with a pitched roof. The houses are settled to the regular blocks divided by intersections (see scheme on Figure 2). Model has been scaled down to 1 : 200. With respect to the dimensions of test-section, the building height is 7% of test-section height and length of street is 40% of tunnel width.

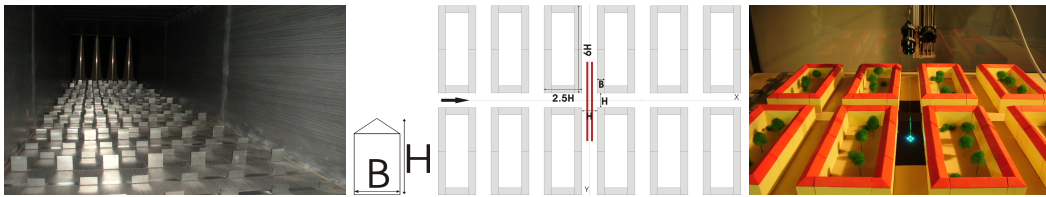


Figure 2: Left: roughness elements in testing section. Right: Scheme of building, model and photograph from experiment. Red lines denote the line source.

Flow characteristics inside the tunnel

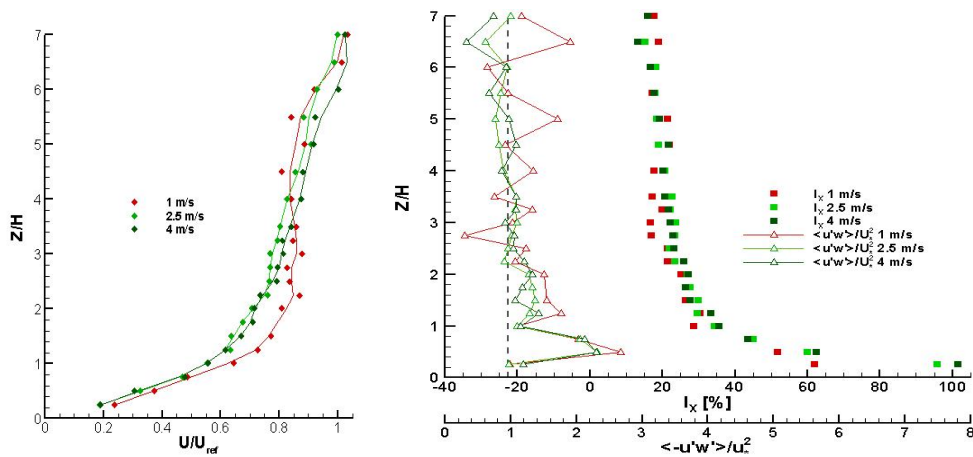


Figure 3: Left: U-components of velocity. Right: turbulence intensity and vertical Reynolds stress.

The vertical profile of turbulent characteristics was measured on three different reference velocities: $1 \text{ m}\cdot\text{s}^{-1}$, $2.5 \text{ m}\cdot\text{s}^{-1}$ and $4 \text{ m}\cdot\text{s}^{-1}$. Close similarity of profiles with two higher reference velocities is apparent

from plots of dimensionless u-component, turbulence intensity and Reynolds stress $\langle u'w' \rangle$ (Figure 3). This similarity suggests that Thowson hypothesis about mean dimensionless turbulent characteristics independence is satisfied for velocity greater than 2.5 m.s^{-1} . The conclusion should be considered in visualization method that is necessarily performed with a small reference velocity. The our experiment was conducted with reference velocity 4 m.s^{-1} .

We have estimated the thickness of inertial layer from the vertical Reynolds stress profile. The inertial layer is proposed like a region where the variation of Reynolds stress does not exceed 10% (the restriction is weaker than the 5% used by Cheng and Castro (2005, vol. 104)). These requirements are fulfilled within region from $Z/H=2.5$ to $Z/H=5$. For symmetry evaluation purpose the lowest level $Z/H=3$ was chosen. At this height the influence from individual obstacle is negligible and flow reflects integral roughness of the surface beneath. At the same time, this level can influence the flow processes inside the model.

The longitudinal and vertical velocity along the lateral axis is depicted in the Figure 4. The u-component velocity decreases due to drag force close to the tunnel walls. The plots collapsed very well with respect to the central symmetry. The w-component velocity has a negative sign to the lateral distance $Y/H=\pm 6$, where it starts to steeply grow up to the significant positive values. The right side of tube has stronger upward motion near the wall than the left side.

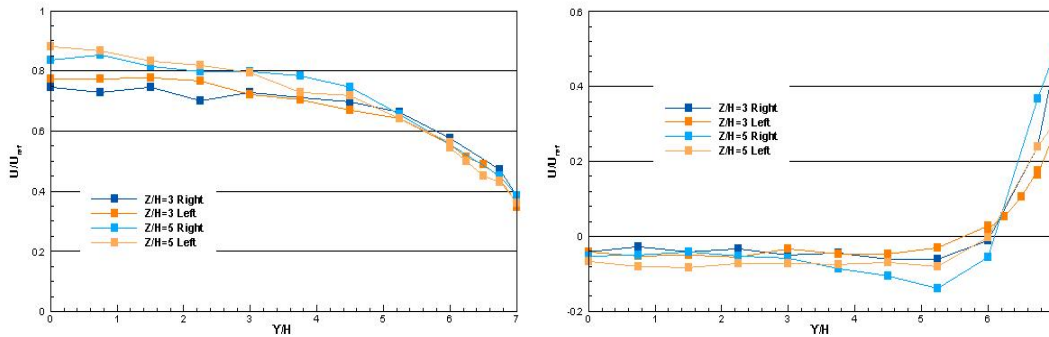


Figure 4: Horizontal and vertical velocity along the lateral axis.

For both components, the symmetry is maintained within the fetch $Y/H=4.5$ from the center. This is confirmed on the base of the same results for root mean squares and for turbulence intensities of u and w components (not shown).

Interesting results are apparent from vertical Reynolds stress plots in Figure 5. The values are axially symmetrical and from negative values at the center they approach the zero value with increasing Y/H . From flow measurement in horizontal plane, the u-velocity shows a symmetry center displacement more

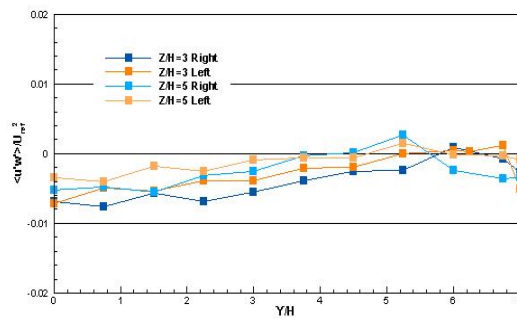


Figure 5: Vertical Reynolds stress along the lateral axis.

closely to the right side by 5% of tunnel width (Figure 6). The lowest level $Z/H=3$ suggests a large outflow on the right side, whereas outflow on the left is much smaller. Next levels upward is situation inverse. An inflow which is fairly symmetrical on both sides comes from wall to the center. Considering the updraft on the outside location at heights $Z/H=3$ and $Z/H=5$, we can suppose that the vertical vortices (vortex

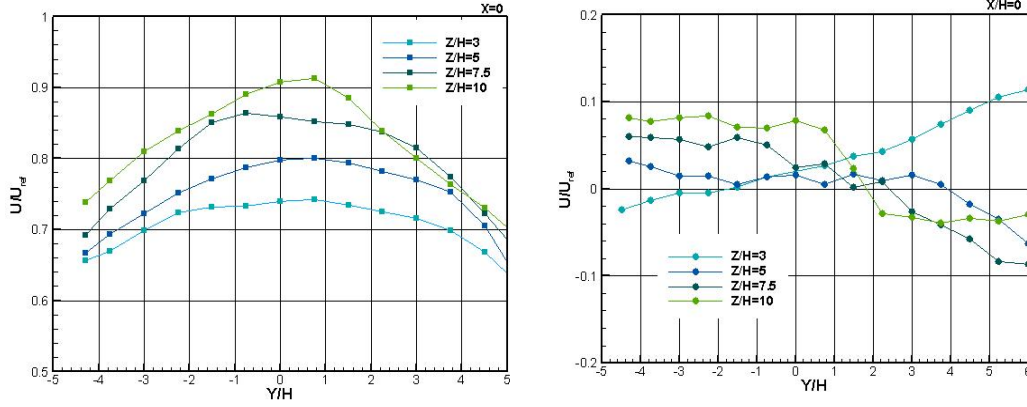


Figure 6: U- and v- components of velocity along lateral axis.

with horizontal axis) are merged between lowest level and upper level. The overall displacement of center of symmetry is 14% to the right side.

Investigation of lateral outflow along the longitudinal x-axis on the side of tube ($Y/H=6$) at various levels found that flow picture is more complex. Figure 7 displays that velocity at each level is exposed to the same process, the v-component of velocity falls down to the maximum inflow and consequently reverses its direction to the significant outflow. The higher level means the later decreasing and increasing. This involves that outflow propagates from ground level upwards. Only highest level $Z/H=10$ shows permanent inflow over the whole section. The u-component gradually increases along the tunnel, whilst

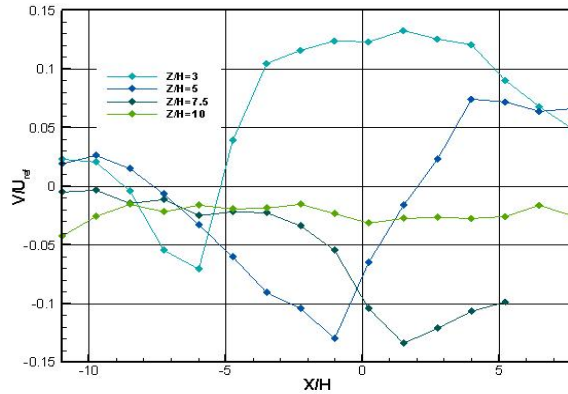


Figure 7: Lateral v-velocity along the longitudinal axis at various level.

w-velocity decreases. This acceleration and deceleration effects are maximum just at the level $Z/H=3$. In the layers above the regression slope falls down to 0.006, that brings a systematic difference in u-velocity $0.12m.s^{-1} \approx 5\%$ between upstream and downstream edge of testing section. The lower layers have a nearly constant plots due to presence of the model. The difference in the turbulence intensity in x-direction between the edges is 2.5%.

Flow characteristics inside the model

In a case with presence of model, the problem whether the internal roughness layer is fully developed above measuring position has been investigated. Under neutrally stratified conditions, the vertical profiles of turbulent characteristics were measured in the central street, parallel with incoming flow (Figure 8).

The strong similarity of profiles of velocity and Reynolds stress in the position B_0, C_0 and D_0 above level $1.5 H$ suggests that internal boundary layer above these positions has very close turbulent characteristics. Further, requirements for equilibrium of canopy sublayer, e.g. layer below the roof level, is

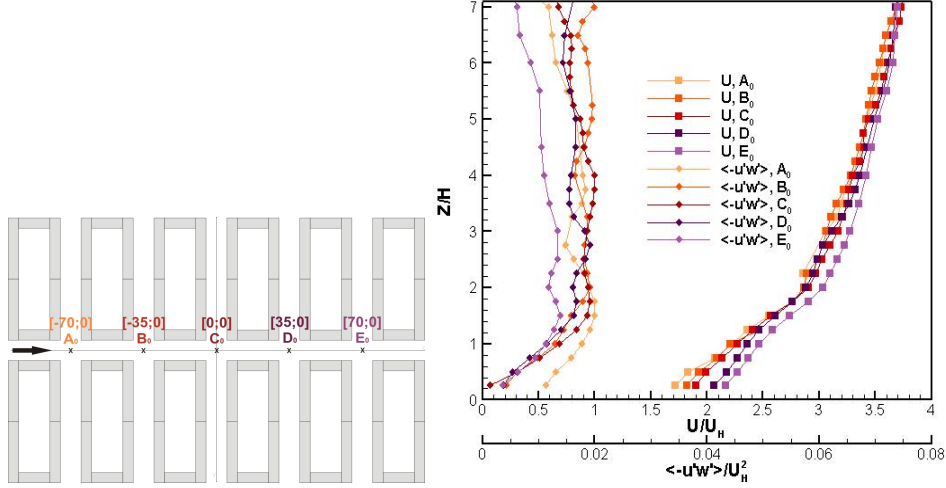


Figure 8: Velocity and vertical Reynolds stress. The positions are denoted in the sketch.

satisfied in the second or the third row of obstacles. Hence, the third row was chosen for experimental purpose.

Upstream outer position A_0 has a different behaviour. Up to the $1.5 H$ level, Reynolds stress values are higher than at another ones. It can be explained by transformation of flow characteristics after reaching the roughness change on its way. The shear stress profile that is generated over the roughness elements has typical enhanced values at the elements height H_E . When flow reaches the roughness step change and enters into central street, Reynolds stress begins to decrease. The change comes from surface level upward.

Within the urban canopy at the same time the velocity profiles indicate the gradually acceleration of u -component along the central street, so-called diffusion effect.

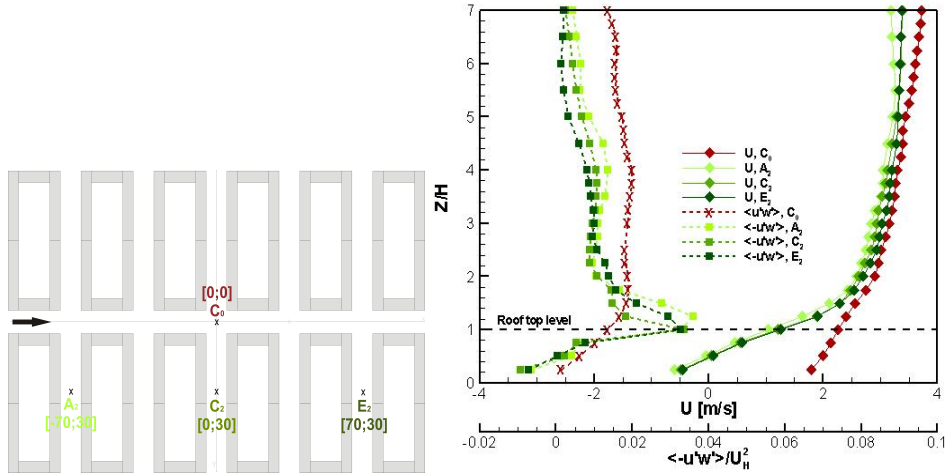


Figure 9: Velocity and vertical Reynolds stress. Position are denoted in the sketch.

One finding can be gained from comparison of vertical profiles above the central street and corresponding street canyons (Figure 9). The vertical Reynolds stress above position C_0 has the greater negative values relative to the position A_2, C_2 and D_2 . The difference at $Y/H=0$ and $Y/H=3$ corresponds to the plot of Reynolds stress at level $Z/H=3$ depicted in the Figure 5.

The spatially averaged velocity data were fitted by the logarithmic and power law. Roughness length and displacement were obtained from shear stress values within the inertial and partially roughness sub-

layer (adopted from Cheng and Catro (2002, vol. 104)). The exponent α was determined by fitting the power law:

Roughness length $z_0 = 3,96$ mm

Displacement $d_0 = 17$ mm

Power law exponent $\alpha = 0,24$

Within the urban canopy ($Z/H=0.75$), inside the central street flow the velocity gradually increases with longitudinal distance (Figure 10 - left). On the entry of the model, the velocity grows explosively due to flow convergence and immediately drops down. In agreement with Cheng and Castro (2002, vol. 105) the stress $\langle u'w' \rangle$ varies with longitudinal fetch. The variation has wave character with wave length equivalent to the pattern length $X/H=3.5$. Over the house block the stress descends to minimal value, whereas it ascends to its maximum above the canyon. Values of velocity fluctuation can be analyzed by

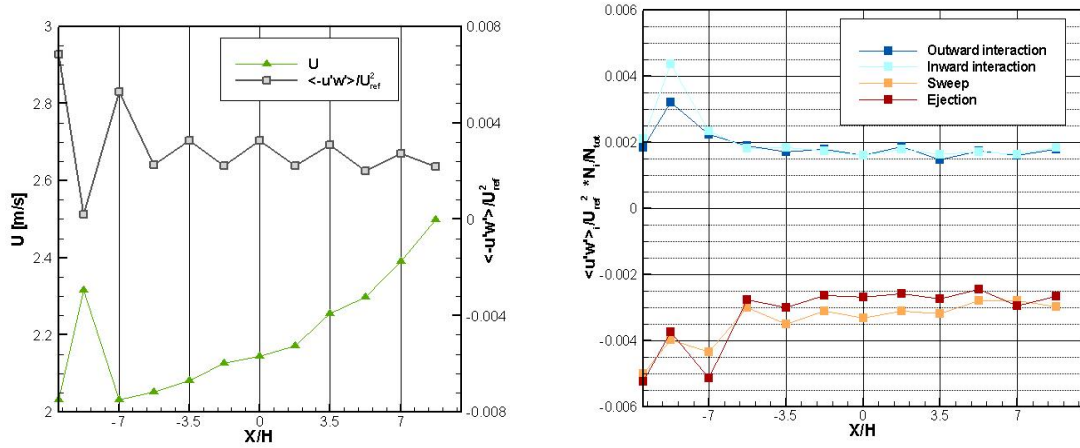


Figure 10: Left: wave variation along the longitudinal axis. Right: Quadrant analysis of vertical Reynolds stress along the lateral axis.

the Quadrant analysis technique. Depending on positive or negative deviation from the velocity average for both flow components u and w , we can establish four quadrants:

$u' > 0, w' > 0$ = 1. quadrant - outward interaction, $u' > 0, w' < 0$ = 2. quadrant - sweeps, $u' < 0, w' < 0$ = 3. quadrant - inward interaction, $u' < 0, w' > 0$ = 4. quadrant - ejection.

The partial contribution from i -th quadrant to the total Reynolds stress $\langle u'w' \rangle$ was obtained from formula of weighted average:

$$\tau_i = \frac{\langle u'w' \rangle_i \cdot N_i}{N_{total}}$$

where $\langle u'w' \rangle_i$ means averaged stress within the i -th quadrant, N_i is the number of events belonging to the i -th quadrant and N_{total} is the global number of events recorded during time period.

The contribution of stress' i - th component is depicted on Figure 10 - right. Slight variations of components, when superposed, form a pronounced final variation. The momentum flux pulses on its way along the central street.

The lateral profile of flow characteristics is displayed in Figure 11. For both components the right side has a slightly higher values, then the left side. It can be explained from the Figure 6, the inlet conditions have stronger longitudinal velocity and more significant outflow on the right side. The approaching flow have certain influence on the condition in the canopy layer, although the model has a dominant role.

Finally, the measurement of w -component velocity and vertical Reynolds stress was done. Surprising results are shown in the Figure 12. The values are strongly asymmetrical.

This asymmetry was investigated with great effort. The first was researched if the asymmetry correspond to the angle between model axis and approaching flow. Various arrangements with fine step (0.2°) were measured. The influence of model's turning was detectable, but still very soft to be able to explain such a difference. Then the all asymmetrical objects on the model, e.g. trees and bushes in the court was removed. The results have not any notable changes. Further, the model was widened just to the walls of tunnel in order to suppress the lateral flow, which could be asymmetrical due to various distance

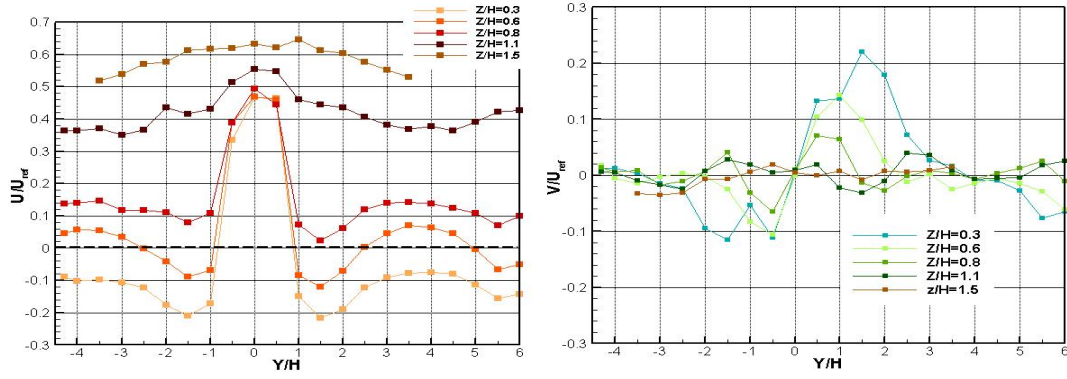


Figure 11: Lateral profiles at various level. Left: u-component. Right: w-component

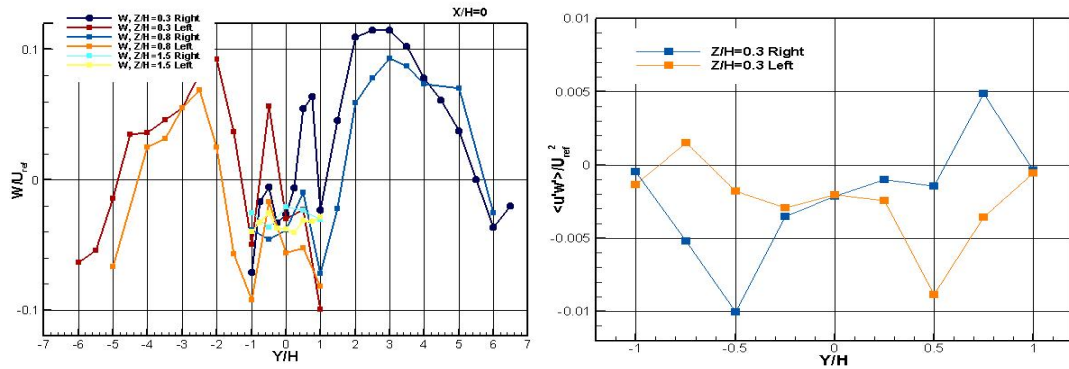


Figure 12: Left plot: velocity w along the lateral axis at various height. Right plot: Vertical stress along lateral axis at $Z/H=0.3$. Left means that probe is looking to the left side, right means inverse direction.

of model from side walls. The widening induced the amplification of the asymmetrical effects, since the flow dominantly flushed through the central street.

Finally, it was discovered that the values are affected by probe mounted on the left or right side (regarding to measuring point). Probe is situated upright to the tunnel axis with distance more then 30 cm from the measuring position. The probe itself has a diameter 6 cm and its front side has an adapter with an aerodynamic shape. But with the probe on the left side the results are strictly symmetrical to them, that we obtained with the probe on the right side. The influence of probe is very significant. The slight discrepancies in the central symmetry of two probe's set-up could be explain by another minor factors like orientation of model to an approaching flow, etc.

From plot 12 - left it is obvious that with increasing height the influence of probe-body on the circumfluence becomes weaker. When the studying position is too much low, the probe is located near the rooftop level. The circumfluence has not many ways how to flow around. The presence of the body force the air flow into central street essentially differently.

Conclusion

The flow quality in aerodynamic low-speed tunnel was investigated. Main objective was the central symmetry. The area proper for a experimental purpose is located within inner 60% of tunnel width. Nevertheless, although the model has dominant force for flow character up to the level $Z/H=1.5$, the asymmetrical inlet conditions could have an influence on experimental results. In our case, the right side of tunnel indicates higher longitudinal velocity and lateral outflow, especially in the middle of working section. And data sets from model measuring inside the canopy layer confirmed the enhanced value of these quantities.

The mild asymmetry was tested by several arrangements with various orientations of model to the

incoming flow. The changes in orientation have been very fine and no significant influence was detected in results. This could be a optimistic conclusion with respect to the difficulties in manufacturing of geometrically precise models. The suppressing the lateral flow due to widening the model hard upon to the walls of tunnel, in order to eliminate unequal flows from the sides, induced amplification of asymmetry within the central street.

The biggest discrepancies in w-component and $\langle u'w' \rangle$ charts was explained like a dependence of the vertical flow field on the position of measuring LDA facility. This finding makes the reliability of LDA measurements problematic in terms of physical modeling method.

Acknowledgements: This project is supported by AVOZ20760514.

References

- [1] Cheng H., Castro I.P.: Near Wall Flow Over Urban-Like Roughness. *Boundary-Layer Meteorology* 104 (2002): 229–259.
- [2] Cheng H., Castro I.P.: Near-Wall Development After a Step Change in Surface Roughness. *Boundary-Layer Meteorology* 105, (2002), 411- 432.
- [3] Jensen M.: The Model-Law for Phenomena in a Natural Wind, *Ingenioren, Int. Ed.*, vol. 2, no. 4 (1958).
- [4] Snyder, W. H.: *Guideline For Fluid Modeling Of Atmospheric Diffusion* (1981). Meteorology and Assessment Division Environmental Sciences, U.S. Environmental Protection Agency.